Effect of an epitaxial $CoSi_2$ layer on diffusion of B and Sb in Si during annealing and oxidation

A. K. Tyagi, L. Kappius, U. Breuer, H. L. Bay, J. S. Becker, S. Mantl, and H. J. Dietze

Citation: Journal of Applied Physics **85**, 7639 (1999);
View online: https://doi.org/10.1063/1.370566
View Table of Contents: http://aip.scitation.org/toc/jap/85/11
Published by the American Institute of Physics

Effect of an epitaxial $CoSi_2$ layer on diffusion of B and Sb in Si during annealing and oxidation

A. K. Tyagi
Zentralabteilung für Chemische Analysen

L. Kappius[a)]
Institut für Schicht- und Ionentechnik, Forschungszentrum Jülich, D-52425 Jülich, Germany

U. Breuer
Zentralabteilung für Chemische Analysen

H. L. Bay
Institut für Schicht- und Ionentechnik, Forschungszentrum Jülich, D-52425 Jülich, Germany

J. S. Becker
Zentralabteilung für Chemische Analysen

S. Mantl
Institut für Schicht- und Ionentechnik, Forschungszentrum Jülich, D-52425 Jülich, Germany

H. J. Dietze
Zentralabteilung für Chemische Analysen

(Received 3 November 1998; accepted for publication 18 February 1999)

The diffusion of B and Sb in Si, with and without a 20-nm-thick epitaxial $CoSi_2$ layer on top, is investigated, during annealing and oxidation, using doping superlattices (DSLs). $CoSi_2$ layers were grown on Si by molecular beam allotaxy. DSLs were grown by molecular beam epitaxy. They consisted of six spikes with peak concentrations of $10^{18}\,cm^{-3}$(B) and about $10^{19}\,cm^{-3}$(Sb) with peak centers spaced 100 nm apart. The shallowest spike was capped with 100 nm of Si followed by 20 nm of $CoSi_2$. Annealing in pure N_2 and oxidation in pure O_2 were performed at temperatures ranging from 800 to 1200 °C. Concentration depth profiles were measured by secondary ion mass spectrometry. The results showed that the dopant diffusion in Si was markedly different with or without a $CoSi_2$ layer. For specimens without $CoSi_2$ layer, we observed oxidation enhanced diffusion of B and oxidation retarded diffusion of Sb in accordance with the literature. However, the effect of $CoSi_2$ layer was a strong retardation of B diffusion and an enhancement of Sb diffusion. The B diffusivity was retarded by a factor of 2–10 as compared to the thermal diffusivity and by a factor of 20–100 as compared to the corresponding diffusivity for oxidation of Si without a $CoSi_2$ layer. Sb diffusivity was enhanced by a factor of 2 with respect to thermal diffusivity and by about a factor of 5 as compared to the case without a $CoSi_2$ layer. © *1999 American Institute of Physics.* [S0021-8979(99)07210-2]

I. INTRODUCTION

Epitaxial silicides grown on silicon and patterned to nanosized structures provide a new way to silicon nanoelectronics.[1] Nanopatterned epitaxial silicides have superior electrical properties as compared to their polycrystalline counterparts. In nanodevices these properties play an increasingly important role. Amongst the silicides $CoSi_2$ is the favorite candidate for epitaxial growth on silicon because of the good lattice match: It crystallizes in the cubic CaF_2 lattice and has a small lattice mismatch of only 1.2% with respect to silicon. It has a low electrical resistance of 14 $\mu\Omega$ cm and an excellent thermal stability. Poly-$CoSi_2$ is already being used as source, gate, and drain contacts for Si metal–oxide–semiconductor field effect transistor (MOSFET) devices.[2] Despite the promising structural match of $CoSi_2$ and Si, heteroepitaxy of $CoSi_2$ on Si is hampered by a strong tendency of growth of misoriented grains. Therefore special growth techniques have to be applied to produce $CoSi_2$/Si heterostructures.[3–6] Thin epitaxial $CoSi_2$ layers can also be grown by molecular beam allotaxy (MBA).[7] This is a modified molecular beam epitaxy (MBE) method consisting of two steps. First, a silicide precipitate layer embedded in single crystalline silicon is grown by coevaporation of Si and Co. Second, rapid thermal annealing is used to form a single crystalline silicide layer. These layers show a high uniformity, sharp interfaces to the silicon, and an excellent thermal stability of up to 1200 °C. Therefore, these layers can be patterned by local oxidation of silicide (LOCOSI).[8] In this patterning process, similar to the well established process of local oxidation of silicon (LOCOS), the silicide layer is capped by a nitride mask that is patterned by optical lithography. During dry oxidation at temperatures ranging from 900 to 1050 °C, over the unprotected areas of the silicide,

a)Electronic mail: l.kappius@fz-juelich.de

$CoSi_2$ dissociates and SiO_2 is formed. The Co atoms diffuse from the $SiO_2/CoSi_2$ interface to the $CoSi_2/Si$ interface to form $CoSi_2$. Near the edges of the nitride mask the silicide layer thins and finally separates. Two metallic pads electrically separated by Si and SiO_2 with a gap of 50 nm can be produced this way.[9] This patterning process has also been used to fabricate a Schottky-barrier MOSFET with ultrashort gatelength.[9]

At the high temperatures that occur during the LOCOSI process, dopant diffusion takes place in the underlying silicon. Hence for electrical applications of this process, prediction and control of the dopant redistribution becomes crucial. It has been shown[10,11] that during oxidation of silicon, boron diffusivity is enhanced whereas antimony diffusivity is retarded. During silicidation with $TiSi_2$, it is vice versa.[12] This is explained on the basis of perturbation in point defects concentration in silicon matrix caused by oxidation or silicidation process. Point defects play a dominant role in the diffusion of dopants in silicon.[13] Boron has been shown to diffuse via a mechanism where silicon interstitials are involved, antimony by a vacancy-assisted mechanism. Therefore, processing steps that inject interstitials, e.g., oxidation, resulting in interstitial supersaturation and vacancy undersaturation, enhance the boron diffusivity and retard the antimony diffusivity,[10,11] while processes like silicidation that lead to interstitial undersaturation and vacancy supersaturation retard the boron diffusivity and enhance the antimony diffusivity.[12]

The influence of the LOCOSI process on the diffusivity of dopants in the underlying silicon has not yet been investigated. One can assume that during $CoSi_2$ layer formation, like in the case of $TiSi_2$ formation, vacancies are injected into the silicon.

On the other hand, it is known that during oxidation of epitaxial $CoSi_2$ layers only about 75% of the Si atoms, which originate from the dissociation of the silicide at the $SiO_2/CoSi_2$ interface, reacts with oxygen to form SiO_2. The remnant 25% of these Si atoms diffuse to the lower interface leading to a supersaturation of interstitials in the silicon matrix.[14] It is therefore difficult to predict the perturbation in point defect population and how the diffusivity of boron and antimony will change under the LOCOSI process.

A well known method to study the diffusivity of dopants in silicon at different depths from the surface is examining the broadening of dopant marker layers in silicon doping superlattices (DSLs).[15] By observing changes in the diffusivities of boron and antimony in DSLs, the depth profiles of Si interstitials and vacancies were obtained.[10] In the present study, we have used DSLs to investigate the influence of a thin (20 nm)$CoSi_2$ layer on diffusivities of boron and antimony in the underlying silicon during oxidation treatment relevant to the LOCOSI process. The dopant depth profiles were measured by secondary ion mass spectrometry (SIMS). The results showed that the diffusion of boron and antimony in the underlying silicon is strongly influenced by the presence of an epitaxial $CoSi_2$ layer.

II. EXPERIMENT

Specimens were grown in a DCA–MBE system of base pressure 5×10^{-11} mbar.[16] Silicon and cobalt were evaporated by e-beam evaporators while boron and antimony from Knudsen cells. The wafer temperature was measured with a thermocouple. Pressure during evaporation increased to about 5×10^{-9} mbar and the main contribution was due to hydrogen (90%) as observed by the quadrupole mass spectrometer attached to the deposition chamber. The deposition rate and layer thicknesses were monitored by a SENTINEL deposition controller. Surface quality during epitaxy was checked *in situ* with reflection high-energy electron diffraction (RHEED). We used 100-mm-diam phosphorous doped float zone Si (100) substrates of 1000 Ω cm resistivity. The wafers were cleaned by a modified RCA-cleaning procedure.[16] The remnant SiO_2 was removed *in situ* in the MBE chamber by evaporation of 5 nm silicon at a substrate temperature of 780 °C and flux rate of 5 pms^{-1}. Subsequently, a 100-nm-thick Si buffer layer was grown. Boron DSLs consisting of six 10-nm-thick spikes separated by 100-nm-thick Si buffer layers were grown by coevaporation of boron and silicon at a substrate temperature of 600 °C. The 100-nm-thick Si buffer layer was grown at a flux rate of 0.15 $nm\,s^{-1}$. In the boron spikes, the Si flux rate was 0.05 $nm\,s^{-1}$. The temperature of the boron effusion cell during evaporation was 1550 °C resulting in a peak concentration of about $10^{18}\,cm^{-3}$. This concentration was chosen to avoid concentration dependent diffusion. Antimony DSLs also consisting of six 10-nm-thick spikes were grown by low temperature MBE (LTMBE). Antimony and silicon were coevaporated at a substrate temperature of 250 °C. The Si flux rate was 0.05 $nm\,s^{-1}$. The Sb source temperature was kept at 200 °C to obtain a peak concentration of about $10^{19}\,cm^{-3}$. To prevent Sb segregation, subsequently a 10-nm-thick Si buffer layer was grown at a flux rate of 0.05 $nm\,s^{-1}$ at the same wafer temperature. The substrate was then heated to 600 °C and a 90-nm-thick Si buffer layer was deposited at a growth rate of 0.2 $nm\,s^{-1}$. This procedure was repeated six times to have six Sb spikes 10 nm thick and separated by 100 nm of buffer layer. After LTMBE the reflexes of the 2×1 RHEED pattern broadened a little bit, but after heating to 600 °C the same pattern appeared as before LTMBE ensuring good crystal quality of the silicon. To flash off remnant Sb atoms from the surface, the wafer was then heated to a temperature of 800 °C for 15 min. After depositing B or Sb DSLs, a 20-nm-thick $CoSi_2$ layer was grown by MBA. At a substrate temperature of 400 °C, Si was evaporated at a constant flux rate of 0.1 $nm\,s^{-1}$. The Co deposition rate was ramped up to a maximum concentration of 31 at. % and then kept constant. The relative amount of Co in the ramp was 50%. The details of this MBA process are described elsewhere.[16]

Similar B and Sb DSLs specimens were also grown without a $CoSi_2$ layer for comparative experiments. As-grown specimens were analyzed by grazing incidence Rutherford back scattering (RBS) using 1.4 MeV He^+ ions to measure the layer thicknesses and to check the deposition rates. The LTMBE grown Sb DSLs specimens without a $CoSi_2$ layer were also examined by RBS/channelling. The

minimum yield value of 3% ensured good crystal quality of the LTMBE layers.

Specimens of size 8 mm×8 mm were cut from the wafers. B and Sb DSLs specimens without a $CoSi_2$ layer were annealed in pure N_2 at temperatures 850–1200 °C to check the thermal diffusion behavior of B and Sb in Si. Such specimens were also given oxidation treatments in dry O_2 at temperatures 800–1200 °C to examine the oxidation enhanced diffusion (OED) of B and oxidation retarded diffusion (ORD) of Sb in Si. Annealing and oxidation treatments were performed in a rapid thermal annealing (RTA) furnace.

B and Sb DSLs specimens with a $CoSi_2$ layer were annealed at 1050 °C in 90% N_2-10% O_2 for 20 and 30 s, respectively, to form a uniform $CoSi_2$ layer. The B and Sb peaks did not broaden much by this treatment. We used an ambient consisting of 90% N_2 and 10% O_2 as annealing in pure N_2 leads to thermal etching and disintegration of the silicide layer, whereas a small addition of oxygen helps to maintain the uniformity of $CoSi_2$ layer.[17] These specimens were then oxidized in dry O_2 at temperatures 900–1200 °C for times that ensured sufficient broadening of B and Sb peaks. A set of specimens without a $CoSi_2$ layer, pretreated in N_2+O_2 at 1050 °C for 20 s (B) or 30 s (Sb), were also given the same oxidation treatment simultaneously for comparison. Another set of specimens without a $CoSi_2$ layer was pretreated in pure N_2 at 1050 °C for 20 s (B) or 30 s (Sb) and then annealed in pure N_2 at the same temperatures and for the same times as the $CoSi_2$ specimens were oxidized. These last specimens, therefore, got the corresponding thermal budget as the oxidation treatment given to $CoSi_2$ specimens. The sheet resistance of all the $CoSi_2$ specimens was measured using the Van der Pauw method. All specimens showed a sheet resistance of 6.5 Ω/square, independent of their treatment, ensuring that the $CoSi_2$ layers remained stable and uniform during the experiments reported here. This value of sheet resistance corresponds to a specific resistance of 14.3 Ω cm.

B and Sb depth profiles were measured by SIMS using a CAMECA IMS 4F instrument. The secondary ions $^{11}B^+$ and $^{123}Sb^-$ were monitored under 12.5 KeV $O2^+$ and 10 KeV Cs^+ primary ion bombardment, respectively. The primary ion beam was raster scanned over an area of 200 μm ×200 μm whereas secondary ions were collected only from the central of 60 μm diam in order to avoid the crater edge effects. The SIMS craters were examined by DEKTAK surface profiler to measure their depths and to check the surface roughness of sputtered craters. SIMS depth profiles were quantified for B and Sb concentrations using the implantation standards from Charles Evans and Associates, USA.

III. RESULTS

Diffusion coefficients in Si are usually extracted from the measured SIMS depth profiles by solving the diffusion equation with the help of process simulators.[12] However, diffusion of dopant spikes can be described by Gaussian broadening and using the thin-layer solution of the diffusion equation, the diffusion coefficients, D, can be simply derived by

$$D=\frac{W^2-W_0^2}{4t}, \tag{1}$$

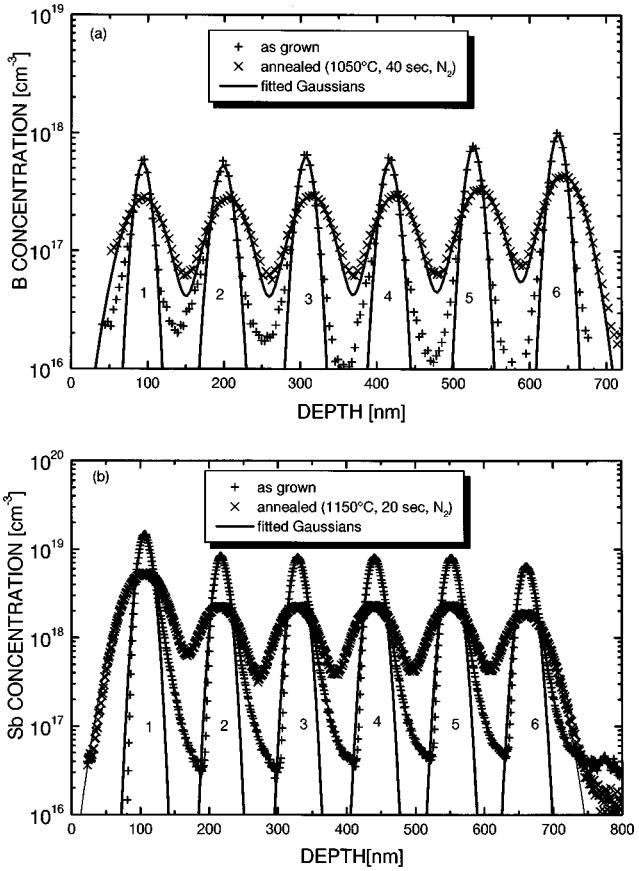

FIG. 1. SIMS depth profiles of (a) B- and (b) Sb-doping superlattices in Si. Specimen and treatment details are given in the inset. Spikes are marked as 1–6. Also shown by the solid line curves are fitted Gaussians to the six spikes.

where W_0 and W are full widths at half maximum (FWHM) of the Gaussian before and after diffusion and t is the time of diffusion.[18] SIMS broadening of the dopant spikes can also be described in first order as Gaussian broadening. This method therefore has the advantage that the instrument related broadening is eliminated during the evaluation of diffusion coefficient. A computer program was written that detected the six B or Sb peaks in the SIMS depth profiles and performed a chi^2-minimization to fit six Gaussians to the measured data.[19] Figure 1 shows representative SIMS depth profiles of B and Sb DSLs in the as-grown and diffused (N_2-annealing) conditions. It is evident that the last B spike and the first Sb spike have a little higher dopant concentration due to the growth process itself. A comparison of the fitted Gaussians (solid lines) and the measured data is also shown. A good conformance is achieved. Each dopant spike after diffusion was analyzed separately by comparing with its corresponding counterpart before diffusion. Diffusion coefficients were evaluated using Eq. (1) for the six dopant spikes. The main sources of errors in determination of diffusion coefficients were uncertainties in depth scale of SIMS profiles and measurement errors in time and temperature of diffusion treatments. The depth calibration of SIMS profiles was performed using the sputter rate calculated on the basis of crater depth measurements by DEKTAK surface profiler as well as estimates based on measurements of ion implan-

TABLE I. Summary of experimental results.

Specimen	Pretreatment	Diffusion treatment	D/D_{int}
B DSLs in Si	1050 °C, 20 s, N_2+O_2	900 °C, 14 min, O_2	0.21
with a $CoSi_2$ layer	1050 °C, 20 s, N_2+O_2	950 °C, 6 min, O_2	0.28
	1050 °C, 20 s, N_2+O_2	950 °C, 3 min, O_2	a
	1050 °C, 20 s, N_2+O_2	1000 °C. 1 min, O_2	0.53
	1050 °C, 20 s, N_2+O_2	1050 °C, 20 s, O_2	0.56
	···	1050 °C, 20 s, N_2+O_2	0.75
	···	1050 °C, 40 s, N_2+O_2	0.52
	···	1100 °C, 20 sec, N_2+O_2	0.80
B DSLs in Si	1050 °C, 20 s, N_2+O_2	900 °C, 14 min, O_2	a
without a $CoSi_2$ layer	1050 °C, 20 s, N_2+O_2	950 °C, 3 min, O_2	a
	1050 °C, 20 s, N_2+O_2	1000 °C, 1 min, O_2	a
	1050 °C, 20 s, N_2+O_2	1050 °C, 20 s, O_2	a
	···	800 °C, 15 min, O_2	1.43
	···	850 °C, 10 min, O_2	7.63
	···	900 °C, 5 min, O_2	1.60
	···	950 °C, 30 s, O_2	3.12
	···	950 °C, 90 s, O_2	4.24
	···	1000 °C, 40 s, O_2	4.20
	···	1050 °C, 10 s, O_2	1.38
	···	1050 °C, 20 s, O_2	4.65
	1050 °C, 20 s, N_2	900 °C, 14 min, N_2	
	1050 °C, 20 s, N_2	950 °C, 3 min, N_2	
	1050 °C, 20 s, N_2	1000 °C, 1 min, N_2	
	1050 °C, 20 s, N_2	1050 °C; 20 s, N_2	
Sb DSLs in Si	1050 °C, 30 s, N_2+O_2	1050 °C, 3 min, O_2	2.11
with a $CoSi_2$ layer	1050 °C, 30 s, N_2+O_2	1050 °C, 6 min, O_2	1.87
	1050 °C, 30 s, N_2+O_2	1050 °C, 9 min, O_2	2.17
	1050 °C, 30 s, N_2+O_2	1100 °C, 1 min, O_2	2.07
	1050 °C, 30 s, N_2+O_2	1100 °C, 2 min, O_2	1.49
	1050 °C, 30 s, N_2+O_2	1150 °C, 20 s, O_2	1.52
	1050 °C, 30 s, N_2+O_2	1200 °C, 5 s, O_2	1.05
	1050 °C, 30 s, N_2+O_2	1200 °C, 10 s, O_2	1.53
	···	1050 °C, 30 s, N_2+O_2	3.90
	···	1150 °C, 20 s, N_2+O_2	1.83
	···	1200 °C, 20 s, N_2+O_2	
Sb DSLs in Si	1050 °C, 30 s, N_2+O_2	1050 °C, 3 min, O_2	a
without a $CoSi_2$ layer	1050 °C, 30 s, N_2+O_2	1050 °C, 9 min, O_2	a
	1050 °C, 30 s, N_2+O_2	1100 °C, 20 s, O_2	a
	1050 °C, 30 s, N_2+O_2	1150 °C, 2 min, O_2	a
	1050 °C, 30 s, N_2+O_2	1200 °C, 5 s, O_2	a
	1050 °C, 30 s, N_2+O_2	1200 °C, 10 s, O_2	a
	···	1050 °C, 16 min, O_2	0.33
	···	1100 °C, 4 min, O_2	0.26
	···	1100 °C, 9 min, O_2	0.24
	···	1150 °C, 3 min, O_2	0.13
	···	1200 °C, 20 s, O_2	0.42
	1050 °C, 30 s, N_2	1100 °C, 2 min, N_2	
	···	1150 °C, 20 s, N_2	
	···	1200 °C, 5 s, N_2	
	···	1200 °C, 10 s, N_2	

[a]Indicate runs for which broadening of the spikes was to small to evaluate the diffusion coefficients.

tation standards and knowledge of thicknesses of deposited layers as monitored during evaporation. However, the accuracy of this depth calibration was ±10%. Total errors in diffusion coefficients reported here are estimated to be about ±30%, unless specifically mentioned for some values. It is worth mentioning that some earlier SIMS experiments, reported in literature, on the influence of silicide layers on dopant diffusion in Si suffered from the roughness of the polycrystalline $CoSi_2$ layers[20–22] whereas in the present study this effect can be excluded due to the excellent smoothness of the epitaxial $CoSi_2$ layers. This was also confirmed by the surface profiler measurements of SIMS craters. The experimental results of the present study are summarized in Table I.

Thermal diffusion data of B and Sb in Si were obtained by annealing the DSLs specimens without $CoSi_2$ layer in pure N_2. The evaluated diffusion coefficients varied in the range 2×10^{-16}–$4\times10^{-13}\,cm^2\,s^{-1}$ for B at temperatures

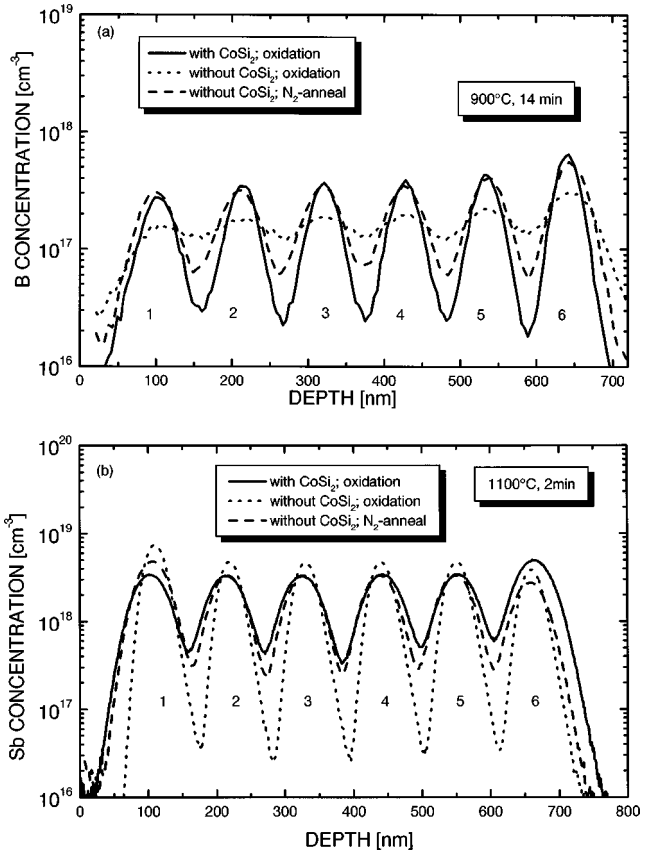

FIG. 2. SIMS depth profiles of (a) B- and (b) Sb-doping superlattices in Si depicting broadening of spikes due to annealing and oxidation. Specimen and treatment details are given in the inset. Spikes are marked as 1–6. The depth scale for the specimen with a $CoSi_2$ layer is adjusted by removing the data points up to a certain depth in order to match the first peaks with other specimens without a $CoSi_2$ layer.

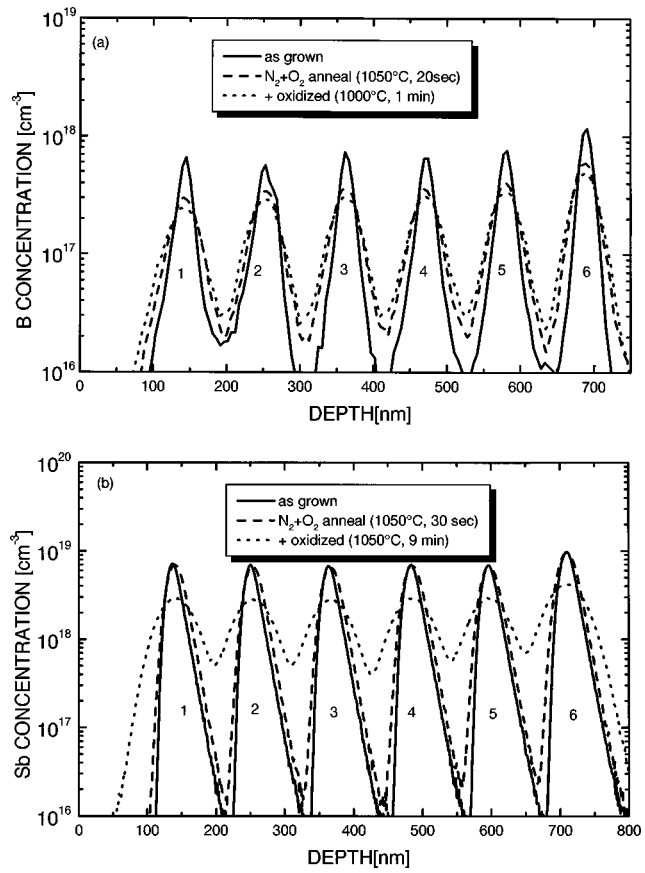

FIG. 3. SIMS depth profiles of (a) B- and (b) Sb-doping superlattices in Si, as-grown, after N_2+O_2 anneal for layer formation and after subsequent oxidation in dry O_2. Specimen and treatment details are given in the inset. Spikes are marked as 1–6.

850–1150 °C and 2×10^{-15}–2×10^{-13} $cm^2\,s^{-1}$ for Sb at temperatures 1000–1200 °C. The diffusion coefficients obeyed the Arrhenius law. These are in good agreement with the reported values.[23] This also ensured the good quality of the Si epilayers deposited in the present experiments. OED of B and ORD of Sb was observed at temperatures 800–1200 °C, in accordance with the earlier reported results.[10,11] The boron diffusivity was enhanced by a factor of 4–10 and the Sb diffusivity was retarded by a factor of 2–5 with respect to their respective intrinsic thermal diffusivity values in Si. The depth dependence of diffusivity was observed for B, with effect being more pronounced at lower temperatures, whereas no clear evidence for depth dependence of Sb diffusivity was found. These aspects were however not investigated in detail in the present study.

The influence of $CoSi_2$ layer on B and Sb diffusion in the underlying Si during oxidation relevant to LOCOSI process was investigated by comparing specimens with and without $CoSi_2$ layer undergoing the same treatment simultaneously. Typical results are shown in Fig. 2. The solid and the dotted line curves in Fig. 2(a) show depth profiles of B in specimens with and without a $CoSi_2$ layer which were pretreated at 1050 °C for 30 s and then oxidized at 900 °C for 14 min whereas the dashed line is for a specimen without a $CoSi_2$ layer which was both pretreated and then annealed in pure N_2 at the same temperature and for the same times. It is evident that boron diffusion is strongly retarded during oxidation for the specimen with a $CoSi_2$ layer as compared to the specimen without a $CoSi_2$ layer. The diffusivity is even lower compared to the specimen that has undergone only thermal diffusion in pure N_2. One can also notice depth dependence of oxidation enhanced diffusion of B as the shallower spikes are more broadened compared to the deeper spikes in this case (dotted line curve). The opposite effect is seen for Sb in Fig. 2(b) for 1050 °C, 30 s pretreatment and 1100 °C, 2 min diffusion treatment. The spikes in the solid line curve are much more broadened compared to those in the dotted line curve as well as to those in the dashed line curve.

Figure 3(a) shows a representative SIMS depth profile of boron DSLs with a $CoSi_2$ layer that did undergo a treatment typical for the LOCOSI process. It was first annealed in N_2+O_2 at 1050 °C for 20 s to form a uniform $CoSi_2$ layer and afterwards oxidized in dry O_2 at 1050 °C for 20 s. It is evident that B peaks have broadened, although not much, after N_2+O_2 anneal and this profile has to be taken as the initial B profile to determine diffusion coefficients under subsequent oxidation treatment. Similar profile for antimony DSLs with a $CoSi_2$ layer in the as-grown condition, after 1050 °C; 30 s anneal in N_2+O_2 to form the uniform $CoSi_2$ layer and after subsequent oxidation at 1100 °C for 2 min is

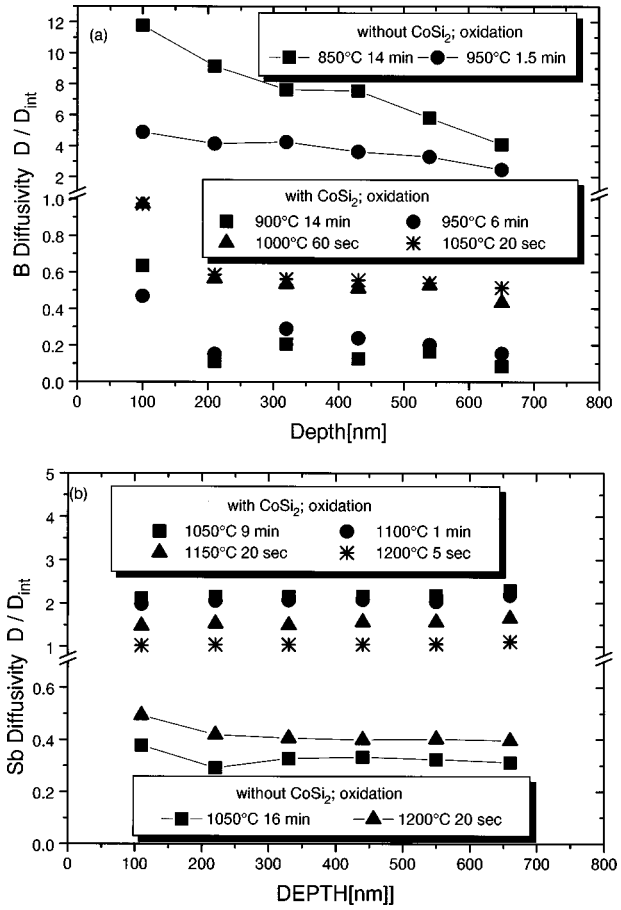

FIG. 4. Normalized diffusivities, D/D_{int}, for B and Sb in Si as a function of depth for oxidation of specimens with and without a $CoSi_2$ layer. Oxidation temperature and time are indicated in the insets.

shown in Fig. 3(b). The Sb peaks did not broaden significantly due to the initial pretreatment in N_2+O_2. This is because of the much lower diffusion of Sb compared to that of B. It is also the reason that we could have 30 s pretreatment for Sb specimens whereas we have to restrict it to only 20 s for B specimens in order to retain good dynamic range of spikes for subsequent oxidation experiments. After pretreatment in N_2+O_2, the $CoSi_2$ specimens were oxidized in dry O_2 at temperatures ranging from 850 to 1200 °C for different times to ensure sufficient broadening of spikes. The B and Sb depth profiles were measured and the diffusion coefficients were evaluated. The results are shown in Figs. 4(a) and 4(b), where the normalized diffusion coefficients are plotted at different depths as evaluated for the six spikes of B and Sb, respectively. For a clearer view, the error bars are not indicated but as stated earlier the error in D values are $\cong$30% except for the 1200 °C 5 s data where the errors were $\cong$50%. It is evident that B diffusivity is retarded strongly by about a factor of 2–10 and Sb diffusivity is enhanced by about a factor of 1.5–2 as compared to their intrinsic thermal diffusivity in Si. The influence is more pronounced at lower temperatures. Also, there is no clear evidence for depth dependence of diffusion coefficients for both B and Sb for specimens with $CoSi_2$ layer. For comparison, in the same Figs. 4(a) and 4(b), we have also shown our results for the oxidation of B and Sb DSLs specimens without a $CoSi_2$ layer (LOCOS process). The opposite effect on dopant diffusivity for oxidation treatments relevant to LOCOS and LOCOSI process can be seen strikingly in Fig. 4.

IV. DISCUSSION

Our experiments have clearly shown that the diffusion of dopants is markedly different in Si with and without a $CoSi_2$ layer. This is true for both, *n*- and *p*-type dopants, antimony, and boron. In the presence of a $CoSi_2$ layer, retardation of boron diffusion and enhancement of antimony diffusion is observed. The boron diffusivity is retarded by a factor of 2–10 as compared to the thermal diffusivity and even more strongly by a factor of 20–100 as compared to the corresponding diffusivity values for oxidation of silicon without a $CoSi_2$ film. Antimony diffusivity is enhanced by about a factor of 2 with respect to thermal diffusivity and by about a factor of 5 as compared to the case without a $CoSi_2$ film. As boron diffusivity is proportional to the relative interstitial concentration and antimony diffusivity is proportional to the vacancy concentration, we can conclude that the local oxidation of the silicide layer leads to an interstitial undersaturation of C_I/C_I^* ranging from 0.15 ± 0.1 to 0.5 ± 0.3 and a vacancy supersaturation of C_V/C_V^* ranging from 1.2 ± 0.2 to 2.4 ± 0.5 for the oxidation treatments used in the present study. Here C_I and C_V are the interstitial and vacancy concentration and C_I^*, C_V^* are the corresponding equilibrium values.

The effect of a $CoSi_2$ film on point defects in underlying silicon has recently been reported by Herner, Gossmann, and Tung.[24] They found enhancement of antimony diffusion and retardation of boron diffusion in silicon with single and polycrystalline $CoSi_2$ films for annealing in N_2 for 1 h at 850 °C. Their results are qualitatively in agreement with our experiments. Quantitative comparison is difficult because first their experiments were performed at lower temperatures and second we used MBA for growth of the epitaxial $CoSi_2$ layer whereas Herner, Gossmann, and Tung used oxide mediated epitaxy. Since they also showed different behavior for single and polycrystalline silicide films, it is apparent that $CoSi_2$ films grown by different techniques may lead to different quantitative results. There are different possible explanations for the origin of the point defect perturbation, the interface can act as source for vacancies or as sink for interstitials. Also macroscopic effects as strain are discussed. Herner, Gossmann, and Tung could show that the interface acts both as source for vacancies and as sink for interstitials. As in our case we are dealing with two effects, the oxidation and the silicidation simultaneously, our data do not give any clue as to which mechanism is the dominating one.

Sb diffusivities did not show a significant depth dependence. This is in agreement with earlier results that indicated that point defects can easily diffuse to the deepest spike resulting in a homogeneous depth distribution of point defects.[25] For the diffusion of boron, a slight depth dependence was observed. Here, the first peak in boron DSLs always showed a higher diffusivity. This may be due to the injection of interstitials from the $CoSi_2$/Si interface during oxidation that recombine deeper in the material with vacan-

cies. But it is difficult to stress this point because of the large error bars in the experimentally measured values. In general, it could be shown that the interstitial undersaturation due to the formation of the silicide layer gave rise to a more pronounced effect than the possible interstitial injection during oxidation.

From a technological point of view, for the application of LOCOSI process in nanotechnology, the present results have a positive impact because the redistribution of boron during the processing steps has always been a serious diffusion problem for devices. The observed retardation of boron diffusion in silicon during LOCOSI process is extremely helpful for device fabrication. On the other hand, a small enhancement of antimony diffusion is tolerable, because the antimony diffusion is fairly slow in silicon any way.

In conclusion, we have shown that oxidation of silicon with a MBA grown epitaxial thin $CoSi_2$ layer at temperatures 900–1200 °C leads to interstitial undersaturation and vacancy supersaturation in the substrate resulting in a retardation of boron diffusion and an enhancement of antimony diffusion. Boron diffusivity is retarded very strongly, as high as by a factor of 20–100, as compared to the case of oxidation of silicon without a $CoSi_2$ layer.

[1] J. R. Tucker, C. Wang, and T.-C. Shen, Nanotechnology **7**, 275 (1996).
[2] K. Maex, Mater. Sci. Eng., R. **11**, 53 (1993).
[3] R. T. Tung, F. Schrey, and S. M. Yalisove, Appl. Phys. Lett. **55**, 2005 (1989).
[4] J. R. Jimenez, L. J. Schowalter, L. M. Hsiung, K. Rajan, S. Hashimoto, R. D. Thompson, and S. S. Iyer, J. Vac. Sci. Technol. A **8**, 3014 (1990).
[5] R. Stalder, C. Schwarz, H. Sirringhaus, and H. von Känel, Surf. Sci. **271**, 355 (1992).
[6] R. T. Tung, Appl. Surf. Sci. **117/118**, 268 (1997).
[7] S. Mantl and H. L. Bay, J. Phys. D **61**, 267 (1992).
[8] S. Mantl, M. Dolle, St. Mesters, P. F. P. Fichtner, and H. L. Bay, Appl. Phys. Lett. **67**, 3459 (1995).
[9] Q. T. Zhao, F. Klinkhammer, M. Dolle, L. Kappius, and S. Mantl, Appl. Phys. Lett. (in press).
[10] H.-J. Gossmann, C. S. Rafferty, H. S. Luftman, F. C. Unterwald, T. Boone, and J. M. Poate, Appl. Phys. Lett. **63**, 639 (1993).
[11] E. Guerrrero, W. Jüngling, H. Pötzl, U. Gösele, L. Mader, M. Grasserbauer, and G. Stingeder, J. Electrochem. Soc. 2181 (1986).
[12] S. B. Herner, K. S. Jones, H.-J. Gossmann, J. M. Poate, and H. S. Luftman, Appl. Phys. Lett. **68**, 1686 (1996).
[13] P. M. Fahey, P. B. Griffin, and J. D. Plummer, Rev. Mod. Phys. **61**, 289 (1989).
[14] F. Klinkhammer, M. Dolle, L. Kappius, and S. Mantl, Microelectron. Eng. **37/38**, 515 (1997).
[15] H.-J. Gossmann, F. C. Unterwald, and H. S. Luftman, J. Appl. Phys. **73**, 8237 (1993).
[16] M. Hacke, Thesis JÜL-3294, ISSN 0944-2952 (1996).
[17] R. Tung and S. Ohmi, Mater. Res. Soc. Symp. Proc. (to be published).
[18] A. K. Tyagi, M.-P. Macht, and V. Naundorf, Acta Metall. Mater. **39**, 609 (1991).
[19] W. H. Press, B. P. Flannery, S. A. Teukolsky, and W. T. Vetterling, *Numerical Recipes in C* (Cambridge University Press, Cambridge, 1988).
[20] J. W. Honeycutt and G. A. Roygonyi, Appl. Phys. Lett. **58**, 1302 (1991).
[21] M. Wittmer, P. Fahey, G. J. Scilla, S. S. Iyer, and M. Tejwani, Phys. Rev. Lett. **66**, 632 (1991).
[22] P. Fahey and M. Wittmer, Mater. Res. Soc. Symp. Proc. **163**, 529 (1990).
[23] R. B. Fair, in *Impurity Doping Process in Silicon*, edited by F. F. Y. Wang (North-Holland, Amsterdam, 1981).
[24] S. B. Herner, H.-J. Gossmann, and R. T. Tung, Appl. Phys. Lett. **72**, 2289 (1998).
[25] T. K. Mogi, M. O. Thompson, H.-J. Gossmann, J. M. Poate, and H. S. Luftman, Appl. Phys. Lett. **69**, 1273 (1996).